# Zebrafish *blowout* provides genetic evidence for *Patched1*-mediated negative regulation of Hedgehog signaling within the proximal optic vesicle of the vertebrate eye

Jiwoon Lee [a], Jason R. Willer [c], Gregory B. Willer [c], Kierann Smith [d], Ronald G. Gregg [c], Jeffrey M. Gross [a,b,*]

[a] Section of Molecular Cell and Developmental Biology and Institute for Cell and Molecular Biology, USA
[b] Institute of Neuroscience, The University of Texas at Austin, Box C1000, 1 University Station, Austin, TX 78712, USA
[c] Department of Biochemistry and Molecular Biology, University of Louisville, Louisville KY, 40202, USA
[d] Department of Molecular and Cellular Biology, Harvard University, Cambridge, MA 02138, USA

## ARTICLE INFO

## ABSTRACT

In this study, we have characterized the ocular defects in the recessive zebrafish mutant *blowout* that presents with a variably penetrant coloboma phenotype. *blowout* mutants develop unilateral or bilateral colobomas and as a result, the retina and retinal pigmented epithelium are not contained within the optic cup. Colobomas result from defects in optic stalk morphogenesis whereby the optic stalk extends into the retina and impedes the lateral edges of the choroid fissure from meeting and fusing. The expression domain of the proximal optic vesicle marker *pax2a* is expanded in *blowout* at the expense of the distal optic vesicle marker *pax6*, suggesting that the initial patterning of the optic vesicle into proximal and distal territories is disrupted in *blowout*. Later aspects of distal optic cup formation (i.e. retina development) are normal in *blowout* mutants, however. Positional cloning of *blowout* identified a nonsense mutation in *patched1*, a negative regulator of the Hedgehog pathway, as the underlying cause of the *blowout* phenotype. Expanded domains of expression of the Hedgehog target genes *patched1* and *patched2* were observed in *blowout*, consistent with a loss of Patched1 function and upregulation of Hedgehog pathway activity. Moreover, colobomas in *blowout* could be suppressed by pharmacologically inhibiting the Hedgehog pathway with cyclopamine, and maximal rescue occurred when embryos were exposed to cyclopamine between 5.5 and 13 hours post-fertilization. These observations highlight the critical role that Hedgehog pathway activity plays in mediating patterning of the proximal/distal axis of the optic vesicle during the early phases of eye development and they provide genetic confirmation for the integral role that *patched1*-mediated negative regulation of Hedgehog signaling plays during vertebrate eye development.

© 2008 Elsevier Inc. All rights reserved.

## Introduction

Vertebrate eye formation commences with the symmetric, bilateral evagination of optic vesicles (OV) from the diencephalon (Adler and Canto-Soler, 2007; Chow and Lang, 2001). Each OV then undergoes a complex series of morphogenetic movements that ultimately results in the formation of a bilayered optic cup, containing the prospective retina and retinal pigment epithelium (RPE). The optic cup remains attached to the diencephalon by the optic stalk, a transient structure that will eventually be filled by retinal ganglion cell axons and form the optic nerve. During optic cup morphogenesis, the neuroectodermal layers of the OV invaginate ventrally and fuse along the proximo-distal axis such that the retina and RPE are confined within the cup. Fusion occurs along a distinct ventral region of the optic cup called the choroid fissure. The choroid fissure is also a transient structure that allows for the exit of retinal axons into the optic nerve, and for the entrance of the hyaloid artery into the eye. Defects in choroid fissure closure result in colobomas; ocular malformations characterized by the persistence of a cleft or hole at the back of the eye (Chang et al., 2006; Fitzpatrick and van Heyningen, 2005; Gregory-Evans et al., 2004). While choroid fissure closure is a critical aspect of ocular development that requires a precise interplay between growth, morphogenesis and regulated gene expression, the molecular and cellular mechanisms underlying this process have not yet been fully elucidated in any vertebrate organism.

Many developmental events in the OV are regulated by secreted signaling molecules of the Bone Morphogenetic Protein (BMP), Transforming Growth Factor Beta (TGF-β), Wnt, Fibroblast Growth Factor (FGF) and Hedgehog (Hh) families (Adler and Canto-Soler, 2007; Chow and Lang, 2001; Esteve and Bovolenta, 2006). Perhaps the best studied of these in early eye development is Hh, whose members regulate several aspects of OV formation, patterning and morphogenesis

(Amato et al., 2004). Sonic hedgehog (Shh), secreted from the ventral midline, first functions in directing the separation of the eye field into two bilateral OVs in both mice and human embryos (Chiang et al., 1996; Roessler et al., 1996). In the zebrafish embryo, mutations in *Shh* do not lead to cyclopia, however, likely due to redundancy with other Hh related proteins (Barresi et al., 2000; Karlstrom et al., 1999; Schauerte et al., 1998). A second key role for Shh signaling in the OV is to promote proximal cell fates (i.e. optic stalk and choroid fissure), and to repress distal cell fates (i.e. retina, RPE and lens). The *pax2* transcription factor is a critical Shh target in this process; *pax2* expression in the optic stalk and choroid fissure is dependent on Shh (Chiang et al., 1996; Perron et al., 2003; Varga et al., 2001; Zhang and Yang, 2001) and *Shh* overexpression is sufficient to induce the expression of *pax2* in more distal OV territories where it is normally absent (Ekker et al., 1995; Macdonald et al., 1995; Perron et al., 2003; Zhang and Yang, 2001). *pax2* and *pax6* repress each other's transcription and thereby form a precise boundary between the optic stalk and retina (Schwarz et al., 2000). Loss of *pax2* function leads to optic nerve hypoplasia and colobomas in human patients, as well as in a number of animal model systems (Macdonald et al., 1997; Otteson et al., 1998; Sanyanusin et al., 1995; Schwarz et al., 2000; Torres et al., 1996).

Zebrafish provide an excellent model system in which eye development can be studied and through which the molecular mechanisms underlying human ocular diseases can be elucidated (Goldsmith and Harris, 2003; Gross and Perkins, 2008). Indeed, loss of function phenotypes for *aussicht*, *pax2a*, *vax1/vax2*, *fgf19*, *n-cadherin*, *apc*, *laminin* β1 and *laminin* γ1 each lead to colobomas in zebrafish and have been informative in furthering our understanding of choroid fissure closure *in vivo* (Heisenberg et al., 1999; Nakayama et al., 2008; Gross and Perkins, 2008). Of particular relevance in this group are the *vax1* and *vax2* genes. The *vax* genes are co-expressed in the optic stalk and ventral optic cup, with *vax1* enriched in the optic stalk and *vax2* enriched in the ventral optic cup (Barbieri et al., 1999; Hallonet et al., 1998; Ohsaki et al., 1999; Take-uchi et al., 2003). Similar to *pax2*, at these early developmental stages, *vax1/vax2* gene expression is also dependent on *Shh* (Perron et al., 2003; Take-uchi et al., 2003), and *Shh* overexpression is sufficient to increase both *vax1* and *vax2* levels (Sasagawa et al., 2002; Zhang and Yang, 2001). Targeted knockout of either *vax1* or *vax2* leads to ventral optic cup defects and colobomas in mouse (Barbieri et al., 2002; Bertuzzi et al., 1999; Hallonet et al., 1999; Mui et al., 2002), and similarly, morpholino disruption of *vax1* and *vax2* results in ventral optic cup defects and colobomas in zebrafish (Take-uchi et al., 2003). The *vax* proteins function in the optic stalk and ventral optic cup by repressing *pax6* expression to promote proximal OV fates over more distal ones (Mui et al., 2005; Take-uchi et al., 2003). Combined, what emerges from these studies is a model in which *Shh* signaling activates *pax2* and *vax1/vax2* pathways, where the *pax2* pathway directly regulates optic stalk and choroid fissure formation while the *vax1/vax2* pathway represses retina and RPE differentiation in the optic stalk and ventral optic cup.

With an interest in better understanding the molecular mechanisms underlying OV morphogenesis and choroid fissure closure, we have positionally cloned and characterized a recessive zebrafish mutant named *blowout* (*blw*), that was originally identified in the large-scale mutagenesis screen in Tübingen (Karlstrom et al., 1996). *blw* mutants possess colobomas and defects in retinotectal projections, although visual function is relatively normal when tested in optokinetic response assays and by electroretinogram (Karlstrom et al., 1996; Neuhauss et al., 1999). Positional cloning of *blw* revealed a nonsense mutation in *patched1* (*ptc1*) as the cause of these ocular defects. Loss of *ptc1* function leads to an expansion of Hh target gene expression in *blw* mutants. Within the OV, *pax2a* expression is expanded distally at the expense of *pax6* and as a result, the optic stalk expands into the ventral optic cup, appearing to physically prevent the lateral edges of the choroid fissure from meeting and fusing. Blocking Hh pathway activity with cyclopamine suppressed colobomas in *blw* mutants indicating that constitutive Hh pathway activity is likely the molecular mechanism underlying the coloboma phenotype in *blw*. These observations highlight the critical role that Hedgehog pathway activity plays in mediating patterning of the proximal/distal axis of the optic vesicle during the early phases of eye development and they provide genetic confirmation for the integral role that *patched1*-mediated negative regulation of Hedgehog signaling plays during vertebrate eye development.

## Materials and methods

### Zebrafish maintenance and strains

Zebrafish (*Danio rerio*) were maintained at 28.5 °C on a 14 h light/10 h dark cycle. Embryos were obtained from the natural spawning of heterozygous carriers or homozygous mutants setup in pairwise crosses. Embryos were collected and raised at 28.5 °C after Westerfield (1995) and were staged according to Kimmel et al. (1995). *blw$^{tc294z}$* outcrosses were provided by Dr. Hans Georg Frohnhöfer at the Max Planck Institute for Developmental Biology and were propagated by repeated outcrosses to TL fish. All animals were treated in accordance with provisions established at the University of Texas at Austin governing animal use and care.

### Histology

Histology was performed as described in Nuckels and Gross (2007). Briefly, mutant and wild-type sibling embryos were collected and fixed overnight at 4 °C in a solution of 1% (w/v) paraformaldehyde (PFA), 2.5% glutaraldehyde and 3% sucrose in phosphate buffered saline (PBS). They were washed 3×5 min in PBS and re-fixed for 90 min at 4 °C in a 2% OsO$_4$ solution, washed 3×5 min in PBS at room temperature (RT) and dehydrated through a graded ethanol series (50, 70, 80, 90, 2×100%). Embryos were further dehydrated 2×10 min in propylene oxide and infiltrated 1–2 h in a 50% propylene oxide/50% Epon/Araldite mixture (Polysciences, Inc.). Embryos were then incubated overnight at RT in 100% Epon/Araldite resin with caps open to allow for propylene oxide evaporation and resin infiltration, embedded and baked at 60 °C for 2–3 days. Sections 1–1.25 μm were cut, mounted on glass slides and stained in a 1% methylene blue/1% borax solution. Sections were mounted in DPX (Electron Microscopy Sciences) and photographed on a Leica DMRB microscope mounted with a DFC320 digital camera.

### Immunohistochemistry

Laminin immunohistochemistry was performed as described in Lee and Gross (2007). Briefly, embryos were collected and fixed overnight at 4 °C in a solution of 4% PFA and 3% sucrose in PBS. Embryos were washed at RT 3×5 min in PBS and processed immediately for whole mount immunohistochemistry. Whole-mount embryos were washed in PBS/0.1% Tween-20 (PBST) and permeabilized 12′ with 100% acetone prechilled to −20 °C. Embryos were washed three times at RT with PBST and digested with proteinase K (10 μg/mL diluted in PBST) for 12–30 min depending on age. Embryos were then washed with PBST, refixed in 4% PFA for 10′ at RT, washed 3× in PBST and blocked for 1 h at RT in block [2% normal goat serum (NGS), 1% DMSO in PBST]. Embryos were then incubated overnight at 4 °C in anti-laminin-111 antibody (Sigma) diluted 1:400 in block. Embryos were washed 5×30′ in PBST and incubated overnight at 4 °C in biotin-SP conjugated affinity purified F(ab')₂ goat anti-rabbit IgG diluted 1:500 in block. Embryos were then washed 5×30′ in PBST and incubated 3 h at RT in Avidin-Peroxidase Complex Reagent (ABC Reagent; Vector Labs). Embryos were washed 3×30′ in PBST and then developed for 10–30′ with DAB reagent (Sigma). After development, embryos were fixed briefly in 4%PFA, cryosectioned and imaged as above. Immunohistochemistry with zpr1, zpr3 and zn8 monoclonal antibodies (Zebrafish International Resource Center) was performed as described by Uribe and Gross (2007). Primary antibodies were diluted at 1:200, Cy3 secondary antibody at 1:300 and Sytox-Green (Molecular Probes) at 1:10,000. Imaging was performed on a Zeiss LSM5 Pascal laser scanning confocal microscope. Three to five optical sections (1 μm in thickness) were collected and projected using Zeiss confocal software. Images were overlaid using Adobe Photoshop CS2.

### 5-Bromo-2-deoxyuridine (BrdU) staining

Embryos were dechorionated and incubated in fish water with 10 mM BrdU (Sigma) for defined time periods and either immediately sacrificed or washed three times into fish water and grown for additional periods before sacrifice. Embryos were processed for immunohistochemistry after Uribe and Gross (2007) with the addition of a 10 min incubation in 4 N HCl at 37° prior to blocking to relax chromatin and facilitate BrdU detection. Mouse anti-BrdU was used at a 1:50 dilution and Cy3 anti-mouse secondaries were used at a 1:200 dilution. Nuclei were counterstained with Sytox-Green (1:10,000; Molecular Probes). Imaging was performed on a Zeiss LSM5 Pascal laser scanning confocal microscope. Three to five optical sections (1 μm in thickness) were collected and projected using Zeiss confocal software. BrdU positive cells and nuclei were counted in three to five eyes from different embryos and averages were compared by Fisher's exact test for statistical significance (Graphpad Prism).

*Positional cloning*

Mapping was essentially performed as in (Willer et al., 2005). A mapping panel was generated by outcrossing a TL+/*blw* with a WIK +/+ fish and then backcrossing a resulting WIK+/*blw* male with a TL+/*blw* female. Genomic DNA was isolated from homozygous embryos and wild-type siblings and used for bulk segregant analysis. Simple sequence length polymorphisms (SSLPs) roughly 20 cM apart across the genome were amplified by PCR and analyzed on E-Gel 4% agarose gels (Invitrogen). Once linkage was detected, 96 individual mutants were genotyped to confirm linkage and refine the interval. For high-resolution mapping, new mapping panels were created by back-crossing two individual WIK+/*blw* females to TL+/*blw* males to create homozygous mutants. Flanking markers Z11410 and Z13521 were used to genotype a total of 526 mutant embryos. The Ensembl Zv6 Zebrafish assembly was used to identify completed BAC sequences in the interval and new markers were designed within these BACs using the Zebrafish SSR search Web site (http://danio.mgh.harvard.edu/markers/ssr.html). A 917 kb critical interval was identified and the open reading frames (ORFs) from six candidate loci in the interval were cloned and sequenced from *blw* and wild-type embryos using Big-Dye chemistry and an ABI 3130XL DNA sequencer (Applied Biosystems). Mutations in *atp6v0b* (NM_199561) and *ptc1* (NM_130988) were identified. A *ptc1* mutation in *blw* was first reported by Koudijs et al. (2008). Confirmation of the identified T→A mutation at position 520 in *atp6v0b* was obtained by genotyping genomic DNA from mutant, WIK+/*blw*, and TL+/*blw* fish using an SNP assay run on a PSQ HS 96 Pyrosequencer (Biotage AB). Confirmation of the identified G→A mutation at position 3119 in *ptc1* was obtained by PCR amplifying the corresponding region of genomic DNA from mutant, WIK+/*blw* and TL+/*blw* fish and then direct sequencing. G3119A also disrupts a conserved *Ava*II restriction site enabling *blw* mutants to be genotyped by restriction fragment length polymorphism (RFLP) assays where genomic DNA was isolated from embryos and a region of the *ptc1* gene from Exon 16 (5′-CCA TGA TAA GTA CGA CAC CAC TGG AGA G-3′) to Intron 17 (5′-CAC TAC ACC AAA TCC CTG ATG GAT GG-3′) spanning the mutation was PCR amplified, gel purified, digested overnight with *Ava*II and analyzed on a 2% agarose gel.

*Morpholino, mRNA and BAC injections*

*ptc1* and *atp6v0b* morpholinos (MOs) were purchased from Open Biosystems (Huntsville, AL). MOs were resuspended in water and injections performed at the 1-cell stage into wild-type Oregon AB embryos. A standard control morpholino (5′-CCT-CTTACCTCAGTTACAATTTATA-3′) was used for injection control embryos and 13 ng was injected. *Ptc1*MO (5′-CATAGTCCAAACGGGAGGCAGAAGA-3′) targeted the translation initiation site of the *ptc1* transcript (Wolff et al., 2003) and 1.3 ng was injected into 1-cell stage wild-type Oregon AB embryos. *atp6v0b* MO (5′-AAGGTTTTATTAGCACT-TACCGACG-3′) targeted the exon1/intron1 junction of the *atp6v0b* transcript and 13 ng was injected into 1-cell stage wild-type Oregon AB embryos. Splicing was verified by RT-PCR as described by Gross and Dowling (2005). For mRNA overexpression, full-length *ptc1* was PCR amplified and subcloned into pCR4-TOPO, and *atp6v0b* and *atp6v0b$^{N113K}$* were PCR amplified and subcloned into pCS2. Plasmid containing cDNAs were linearized and used for *in vitro* translation (mMessage Machine, Ambion). mRNA was resuspended in water and 50 and 100 pg was injected into embryos derived from *blw$^{+/-}$* × *blw$^{+/-}$*, *blw$^{-/-}$* × *blw$^{+/-}$* crosses and/or 1-cell stage wild-type Oregon AB embryos. BAC DKEY-31M5 was purchased from RZPD (Berlin, Germany), isolated from bacteria (Qiagen) and injected into 1-cell stage embryos derived from heterozygous *blw* incrosses.

*Riboprobes and in situ hybridization*

Hybridizations were performed essentially as described by Jowett and Lettice (1994) using digoxigenin labeled antisense RNA probes. *ptc1* was cloned from 24 hpf cDNA, ligated into pGEM-T and used for probe synthesis (cloning details available upon request). *In situ* hybridizations on embryos younger than 48 hpf were performed on embryos derived from homozygous incrosses such that all embryos were mutant and genotyping was unnecessary. Probe synthesis constructs for the listed genes were generously provided by the following researchers: *pax2a* (Bruce Riley, Texas A&M University), *ptc2* (Brian Perkins, Texas A&M University) and *pax6* (Brian Link, Medical College of Wisconsin).

*Cyclopamine treatments*

Cyclopamine (Sigma) was resuspended at 10 mg/mL in 100% ethanol and diluted into fish water for exposures. Ethanol (100%) was used for vehicle controls. Embryos derived from homozygous *blw* incrosses were used for all exposures. Embryos were removed from cyclopamine at defined times and washed into fish water for further culturing. Cyclopamine rescue data were analyzed by Fisher's exact test for statistical significance (Graphpad Prism).

## Results

*Blowout mutants possess defects in choroid fissure closure*

*blw* mutants present with obvious colobomas (Figs. 1A–D). In mutants, the choroid fissure has not closed and as a result, retinal and RPE tissue are not contained within the eyecup (Figs. 1E–I). Severity of the phenotype varies between homozygous embryos with phenotypes ranging from subtle, unilateral colobomas in some embryos to severe, bilateral colobomas in others. Retinal and RPE tissue extend from the eyecup into the forebrain in the most severely affected mutants (Fig. 1I), while in those less severely affected, a cleft is observed surrounding the choroid fissure but little to no retinal tissue has expelled
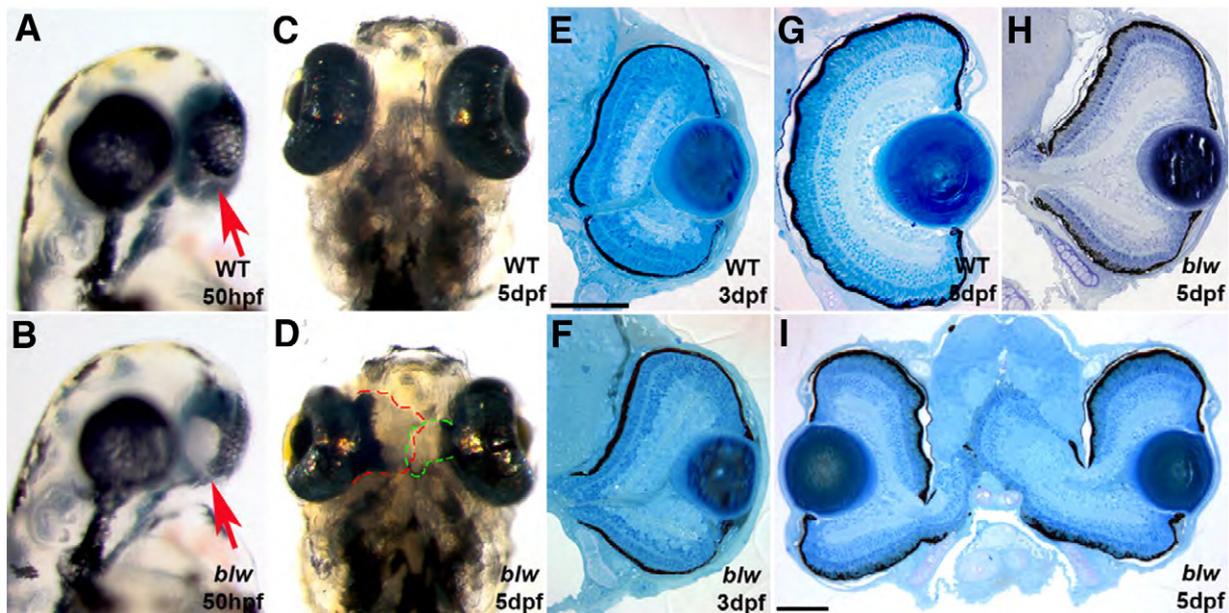


**Fig. 1.** *blowout* mutants present with colobomas. Wild-type (A, C) and *blw* (B, D) mutant embryos at 50 hpf (A, B) and 5 dpf (C, D) imaged laterally (A, B) and ventrally (C, D). Colobomas can be unilateral or bilateral, and these *blw* mutants show bilateral incidence. Arrows in panels A and B point to the choroid fissure. Retinal tissue expelled from each eye has been outlined to illustrate the extent of the coloboma in panels C and D. Transverse histological sectioning of wild-type (E, G) and *blw* (F, H, I) eyes. Colobomas are obvious at 3 dpf in *blw* (F); however, at later time points their severity varies ranging from mild (H) to severe (I). Lens and retinal development appear normal in *blw* mutants. Anterior is up in panels A–D. Dorsal is up in panels E–I. Scale bars are 100 μm.

through this cleft (Fig. 1H). Penetrance of the phenotype also varies between clutches, ranging from 3% to 22% of total embryos in any given clutch derived from heterozygous parents developing a coloboma. Within the eye, beyond these containment defects, other aspects of development and patterning appear normal. Lens and RPE formation are unaffected, retinal lamination is normal and all retinal cell types are present in mutant embryos (Fig. 2 and data not shown). Retinal ganglion cell axons are not bundled at the optic nerve and as a result, the nerve is often split into two or more tracts that exit the eye through the colobomatous choroid fissure opening (Fig. 2D). Indeed, retinotectal pathfinding defects have been previously described for this mutant and these may result from this inability to assemble the axons into a tight bundle as they exit the eye (Karlstrom et al., 1996). Interestingly, the region of the retina that extends from the eyecup and into the forebrain develops photoreceptors with fairly normal outer segment morphology as demonstrated by immunostaining for rhodopsin (Fig. 2E) and red/green cone opsin (Fig. 2F), indicating that apposition to the RPE is not necessary for outer segment morphogenesis.

*Colobomas in blowout are not likely a result of retinal overproliferation or an absence of Bruch's membrane*

Overproliferation within the retinal neuroepithelium has been shown to lead to colobomas (Kim et al., 2007) and thus, we first tested the hypothesis that retinal cells overproliferated in *blw* leading to a rupture of the optic cup, and an expulsion of retinal tissue into the forebrain. Proliferation was assessed using BrdU incorporation assays, and BrdU exposures were performed spanning several time points of development (e.g. 24–36 hpf, 42–48 hpf and 72–96 hpf; Figs. 3A, B and data not shown). BrdU incorporates into DNA during S-phase and serves as a useful readout of cell proliferation over a given time period. Quantification of the number of BrdU positive cells over these exposure periods revealed that they were present in similar numbers and location to those in wild-type siblings (Fig. 3C and data not shown) indicating that that overproliferation of the retina is not likely to underlie the *blw* phenotype.

Basement membrane abnormalities are also known to contribute to colobomas (Gross et al., 2005; Hero et al., 1991; Lee and Gross, 2007), so we next tested the hypothesis that basement membrane defects might underlie the colobomas in *blw*. Bruch's membrane is a retinal basement membrane that separates the RPE from the chorio-capillaris at the posterior of the eye and thus provides a physical barrier containing the retina and RPE within the optic cup. Laminin-111 protein is highly expressed in Bruch's membrane (Lee and Gross, 2007), so we utilized an antibody against laminin-111 to determine if the Bruch's membrane was present in *blw* mutants. At all time points examined, laminin-111 levels in *blw* were comparable to those in wild-type embryos (Figs. 3D, E). While this observation suggests that Bruch's membrane is unaffected in the mutants, laminin-111 is not expressed in the colobomatous area because the retina and RPE are expelled through this region. Therefore, while Bruch's membrane appears normal in *blw* mutants, we cannot rule out the possibility that there might be lower laminin-111 levels in the region of the choroid fissure and that these reduced levels compromise retinal containment and contribute to the colobomas in *blw*. Additional histological and molecular evidence described below makes this an unlikely scenario, however.

*Optic stalk formation is abnormal in blowout*

In examining DIC images from *blw* mutant retinal cryosections and laminin-111 expression in *blw*, we observed maintenance of the optic stalk in *blw* mutants relative to wild-type embryos in which the optic stalk had degenerated by this time (arrows in Figs. 3B, E). This prompted us to examine abnormalities in optic stalk formation as a potential cause of the colobomas in *blw*. When one closely examines embryos derived from *blw* heterozygous incrosses at very early stages
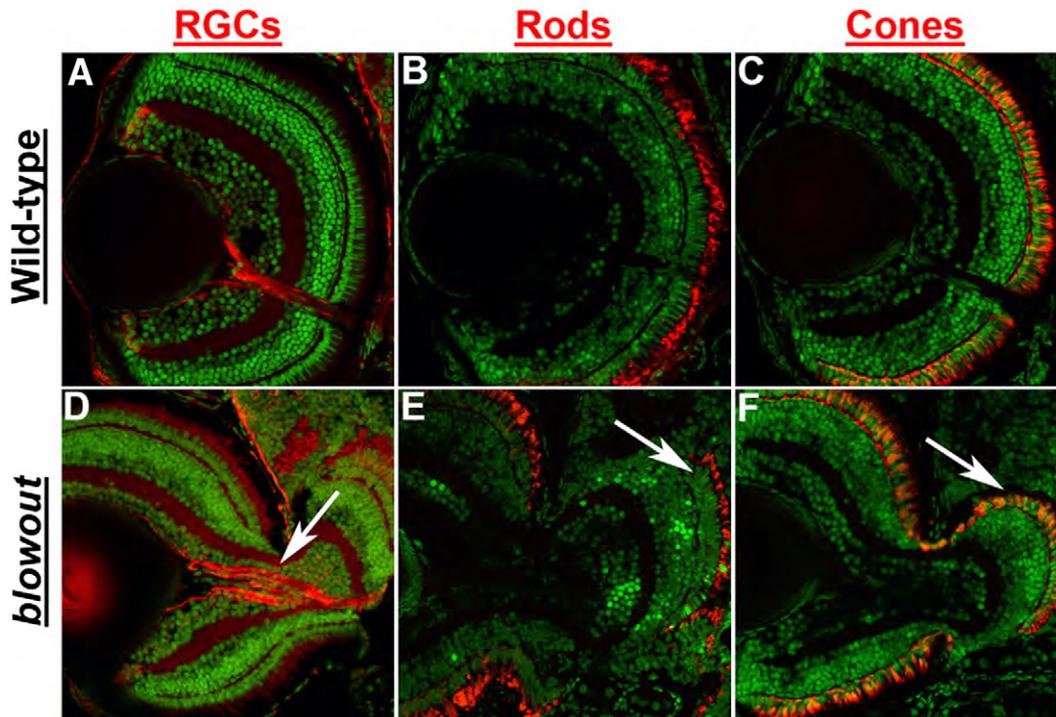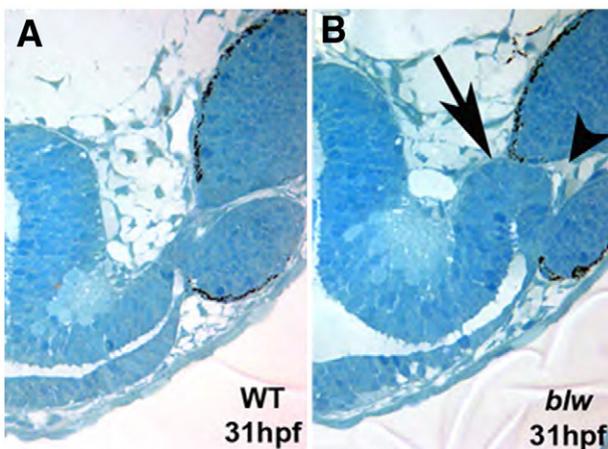


**Fig. 2.** Retinal development is largely normal in *blowout*. Immunohistochemical analysis of retinal ganglion cells (RGCs) via zn8 staining (A, D), rod photoreceptors via zpr3 staining (B, E) and red/green double cones via zpr1 staining (C, F) in transverse retinal cryosections. All retinal cell types are present and are properly distributed in *blw* mutants, and retinal cell numbers are also similar between wild-type and *blw* mutant eyes. RGC organization is affected in *blw* mutants where RGC axons do not assemble into a tight bundle as they exit the eye (arrow in panel D). Photoreceptor outer segments are present in the retinal territories that are not contained within the eye cup (arrows in panels E, F). Antibody stains are red and nuclei are counterstained green with Sytox Green. Dorsal is up in all images.
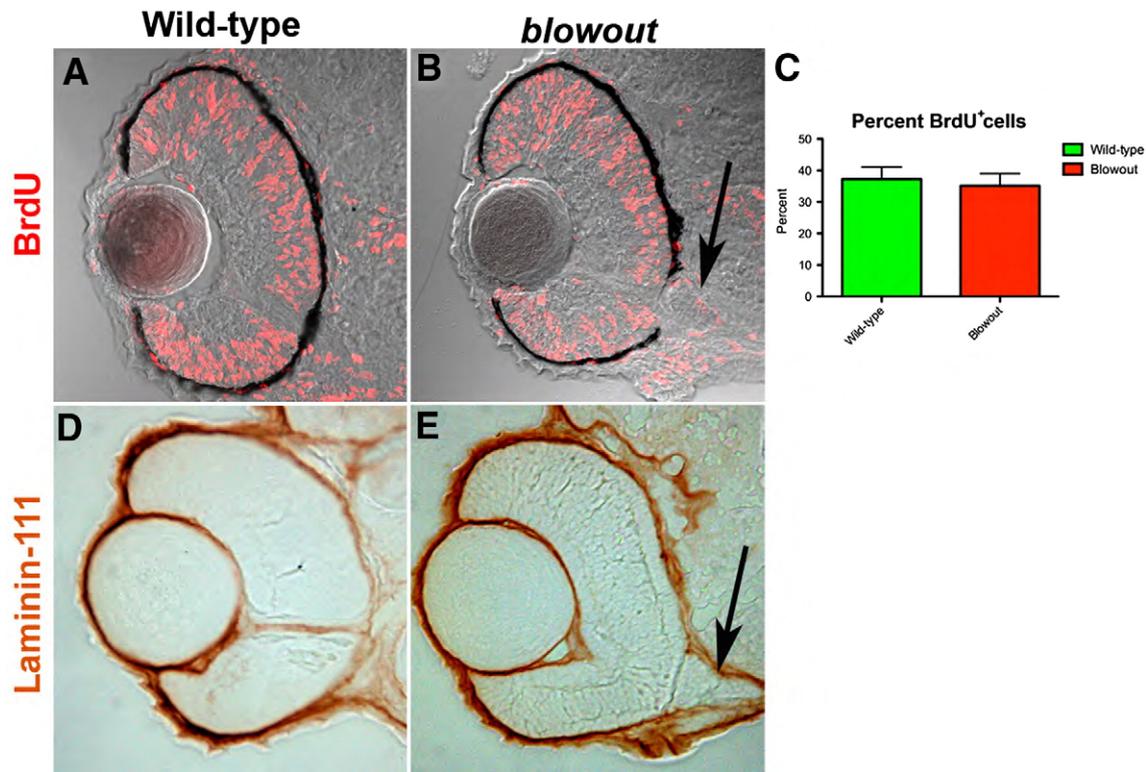
**Fig. 3.** Retinal cell proliferation and Bruch's membrane formation are both normal in *blowout*. (A, B) Wild-type (A) and *blw* (B) embryos were exposed to BrdU from 42 hpf to 48 hpf and immediately sacrificed. BrdU positive cells (red) are observed throughout the retinas of wild-type and *blw* mutant embryos in similar proportions (C; no statistical difference—Fisher's exact test). Additional exposure periods (24–36 hpf, 72–96 hpf) resulted in identical regions of proliferation in the retinas of wild-type and *blw* mutants (data not shown). (D, E) Bruch's membrane, a basement membrane at the posterior of the eye, highly expresses the laminin-111 protein (Lee et al., 2007). Shown here are images of 12 μm cryosections from wild-type (D) and *blw* (E) whole-mount embryos stained for laminin-111 protein at 48 hpf. Laminin-111 levels and distribution are similar between wild-type and *blw* embryos. The optic stalk appears abnormal in *blw*, as it remains connected to the retina at 48 hpf (arrows in panels B, E), while in wild-type siblings it has degenerated. Transverse sections, dorsal is up in all images.

of development (~20–24 hpf), a thicker and expanded optic stalk is observed in a subset of these embryos, suggesting that optic stalk defects might underlie colobomas in *blw* mutants (data not shown). To directly analyze optic stalk formation in *blw*, we performed serial histological sectioning on several mutants and their wild-type siblings at 31 hpf (Fig. 4). By examining serial sections taken at the same plane in both wild-type and *blw* mutants, the optic stalk appeared to be larger in the mutants than that in wild-type siblings (Fig. 4B). More-
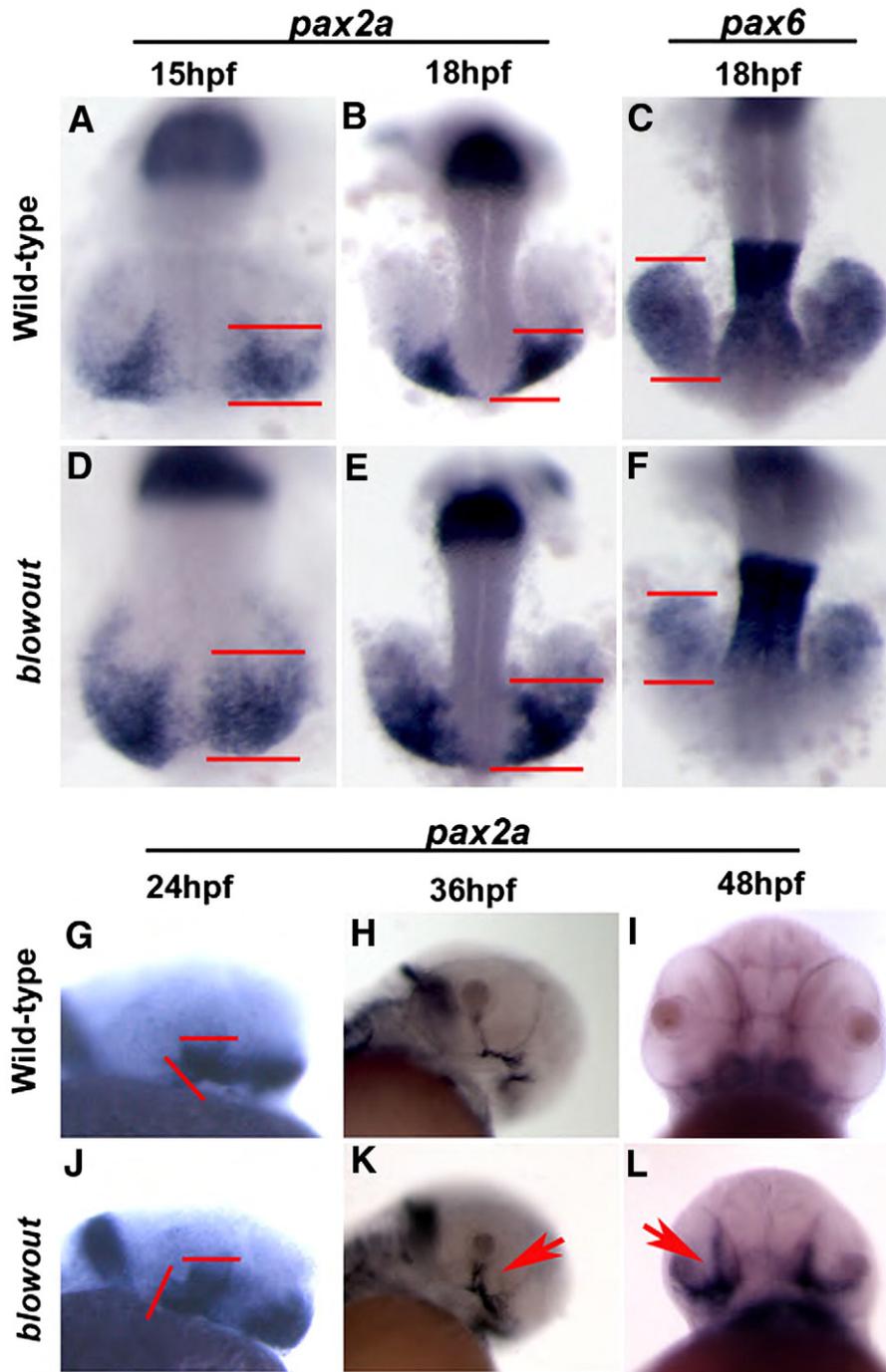
over, the optic stalk was kinked, and stalk tissue was ectopically located within the choroid fissure, appearing to physically prevent the fusion between its lateral edges (arrow in Fig. 4B).

We wanted to further examine the optic stalk phenotype in *blw* to determine if optic stalk defects also manifest molecularly with an expansion of the proximal OV marker *pax2a* and a contraction of the distal OV marker *pax6*, which would suggest shifts in cell fate boundaries within the OV from retina to optic stalk. *pax2a* expression is normally limited to the region of the OV fated to become optic stalk as early as 15 hpf (Fig. 5A) and by 18 hpf, as the OV has fully evaginated from the diencephalon, *pax2a* expression clearly demarcates the optic stalk territory of the OV from the remainder of the OV (Fig. 5B). In *blw* mutants, the *pax2a* expression domain has expanded more distally into the remainder of the OV (Figs. 5D, E) suggesting that proximal OV fates are expanded at the expense of distal ones. Indeed, the *pax6* expression domain is contracted in *blw* mutants in a pattern complementary to the expansion of *pax2a* (Figs. 5C, F). This observation strongly suggests that proximal/distal patterning of the OV is disrupted in *blw* mutants during the early phases of eye development.

*pax2a* also serves as a useful marker of the optic stalk at 24 hpf (Fig. 5G) and 36 hpf (Fig. 5H). In *blw* mutants, the *pax2a* expression domain has substantially expanded and now extends into the retina (Figs. 5J, K). Moreover, while *pax2a* expression is nearly absent from the wild-type eye at 48 hpf, concomitant with optic stalk differentiation (Fig. 5I), in *blw* mutants expression is not only maintained but it also appears to spread into the retina (Fig. 5L). Interestingly, in some embryos, we noted asymmetric changes in *pax2a* expression where one optic stalk would show a large increase and the other would show either a more moderate increase or no change from wild-type levels (data not shown). As stated above, in some *blw* mutants, colobomas are unilateral while in others they are bilateral and thus, it appears



**Fig. 4.** Optic stalk morphology is abnormal in *blowout*. Single 1.25 μm oblique histological sections taken from 31 hpf wild-type (A) and *blw* (B) embryos taken at the same plane of sectioning. The optic stalk in *blw* is larger and kinked at the distal end (arrow in panel B). Optic stalk tissue is present at the choroid fissure and appears to prevent the lateral edges of the fissure from meeting and fusing (arrowhead).

**Fig. 5.** The proximal/distal axis of the optic vesicle is disrupted in *blowout*. *pax2a* marks the proximal OV (optic stalk) in wild-type embryos at 15 hpf (A), 18 hpf (B), 24 hpf (G) and 36 hpf (H), while it is absent at 48 hpf (I) owing to the degeneration of the stalk by this time. Expression in *blw* mutants is observed in a broader domain within the optic stalk region as early as 15 hpf (B) and this expansion is maintained at 18 hpf (E), 24 hpf (J) and 36 hpf (K, arrow). Expression is not extinguished at 48 hpf and can be observed to extend into the retina (L, arrow). Conversely, *pax6* marks the distal optic vesicle (retina and RPE) at 18 hpf (C), and expression is substantially contracted within distal optic vesicle of *blw* mutants (F) in a pattern complementary to the expanded domain of *pax2a*.

that this asymmetry manifests at the molecular level as well as the morphological.

*Positional cloning of blowout*

To enable a molecular characterization of *blw* and its optic stalk phenotypes, we next set out to positionally clone the gene and identify the responsible mutation. Linkage mapping with microsatellite markers placed the mutation on chromosome 2, between Z11410 and Z13521. High-resolution mapping was then performed using addi-

tional microsatellite markers to refine the *blw* locus. Using markers z8451 and CH211-261P7-SSR2, and 526 *blw* mutant embryos, we defined a critical interval that must contain the *blw* locus (Fig. 6A). Assembly of BACs spanning this region identified 10 genes and 1 pseudogene within it (Fig. 6A and data not shown). cDNAs representing six of these genes were cloned and sequenced and, interestingly, separate mutations in two different genes were identified in all 526 *blw* mutant embryos.

The first mutation identified was a missense mutation in *atp6v0b* (NM_199561) that changed bp 520 from T-to-A, resulting in a non-
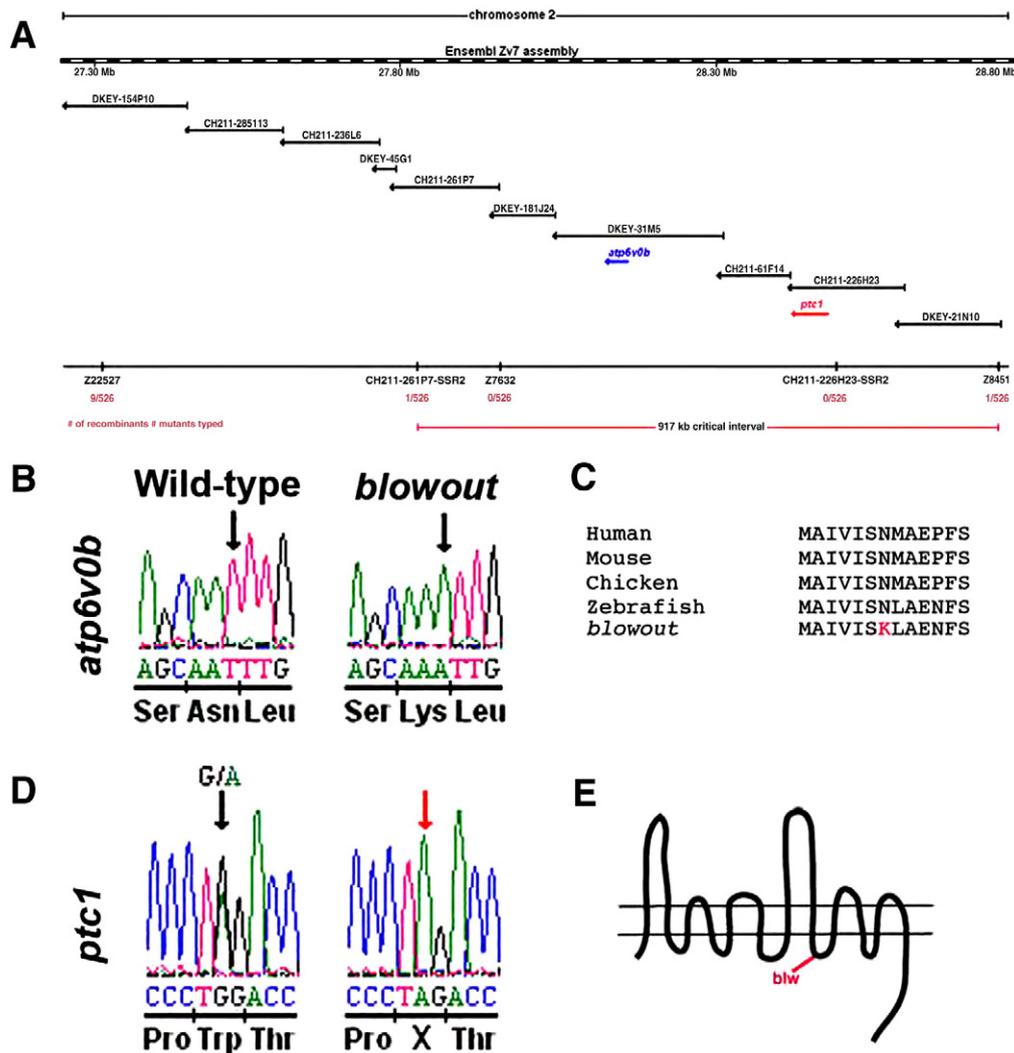
**Fig. 6.** Positional cloning of the *blowout* mutation. (A) Genetic map of Chromosome 2 containing the *blw* mutation. Microsatellite markers and BACs are indicated with the number of recombinants and embryos genotyped. (B) Sequence chromatogram showing the *atp6v0b* mutation in *blw*. DNA sequence from wild-type (left) and homozygous (right) *blw* mutants are shown and the affected base is marked by an arrow. Amino acid sequence is listed below the DNA sequence. (C). Asn113, changed to Lys in *blw* (red), is conserved in vertebrate atp6v0b proteins. (D) Sequence chromatogram showing the *ptc1* mutation in *blw*. DNA sequence from heterozygous (left) and homozygous (right) *blw* mutants are shown and the affected base is marked by an arrow. (E) Schematic of the patched1 protein and the approximate position of the stop codon in *blw* situated after the 8th transmembrane domain.

conservative Asn to Lys change at position 113 of the protein (Fig. 6B; www.ensembl.org/Danio_rerio). *atp6v0b* encodes a 22 kDa proteolipid subunit (v0c″) of the vacuolar ATPase complex (v-ATPase). The v-ATPase is a multi-protein complex consisting of 13 different subunit types that are assembled stoichiometrically into a multimeric protein complex (Nishi and Forgac, 2002). v-ATPases are best known for their roles in H⁺ transport through which they are important for intracellular and extracellular acidification events, protein transport and membrane fusion (Nelson and Harvey, 1999; Nishi and Forgac, 2002). Additionally, several recent studies have identified v-ATPase complex-independent functions for individual v-ATPase subunits (Hiesinger et al., 2005; Kontani et al., 2005), and perhaps the most interesting of these is in *C. elegans* where v0 subunits have been shown to be involved in mediating the release of Hedgehog-like ligands (Liegeois et al., 2006). The v0c″ protein is highly conserved in eukaryotes and prokaryotes and Asn113 is also conserved in vertebrate v0c″ proteins, suggesting that it may be important for protein function (Fig. 6C).

The second mutation we identified in *blw* was a nonsense mutation in *patched1* (*ptc1*; NM_130988) that changes bp3119 from G-to-A, resulting in a premature stop codon at position 1040 of the Patched1 protein (Fig. 6D; http://www.ncbi.nlm.nih.gov/entrez). This truncates Patched1 just after the 8th transmembrane helix (Fig. 6E). Patched1 is a

receptor for Hh ligands and in the unoccupied state, it serves as a negative regulator of Hh signaling by inhibiting the Smoothened protein. Upon binding of a Hh ligand by Patched, inhibition of Smoothened is relieved and a Hh-dependent intracellular signaling pathway begins. Two *patched* genes are found in zebrafish, *ptc1* and *ptc2* (Concordet et al., 1996; Lewis et al., 1999), and *ptc1* is strongly expressed in the optic stalk during the stages of OV morphogenesis (Lewis et al., 1999). Ocular defects have not been described in *ptc1* morphants (Beales et al., 2007; Wolff et al., 2003), and OV morphogenesis does not appear to be disrupted in the zebrafish *ptc2* mutant, *leprechaun* (Koudijs et al., 2005).

*Loss of patched1 function is responsible for the blowout phenotype*

*ptc1* is expressed in the zebrafish optic stalk (Figs. 9A, C) (Lewis et al., 1999), and gene expression therein is known to be dependent on Hh signaling (Macdonald et al., 1995; Take-uchi et al., 2003) making *ptc1* a likely candidate for underlying the *blowout* phenotype. Indeed, that we observe Hh overexpression-like phenotypes in *blw* (e.g. expansion of *pax2a* expression at the expense of *pax6* expression) supports the hypothesis that loss of *ptc1* function may underlie these phenotypes. To determine if loss of *ptc1* function leads to colobomas, we injected a

translation blocking MO targeting the *ptc1* transcript into 1-cell embryos (after Wolff et al., 2003). Knock-down of *ptc1* translation resulted in severe colobomas in all injected embryos, as well as additional overt phenotypes in the eye, brain and muscles (Figs. 7A, B and data not shown). Histological analysis of *ptc1* morphants confirmed the degree to which the eye is affected in these embryos (Figs. 7C–E). Colobomas in *ptc1* morphants were often more severe than those observed in *blw* and the eyes of *ptc1* morphants are rotated laterally relative to wild-type embryos, and their overall position is displaced medially, likely owing to the substantial coloboma and ventral retina defects. Many *ptc1* mutants also showed small, displaced lenses, a phenotype that does not appear in *blw* mutants. The lens phenotype in *ptc1* morphants is identical, however, to that reported to occur as a result of *Shh* overexpression where lens tissue is substantially reduced or absent (Barth and Wilson, 1995; Dutta et al., 2005; Yamamoto et al.,

2004). Unfortunately, rescue experiments via injection of full-length *ptc1* mRNA into *blw* mutants and/or *ptc1* morphants were not successful, possibly owing to the large size of the *ptc1* transcript and/or degradation of the mRNA once injected (data not shown). Thus, the biological relevance of the increased severity of the *ptc1* morphant phenotype remains uncertain. However, and of particular note, molecular changes in *ptc1* morphants are identical to those observed in *blw* mutants where *pax2a* expression is expanded and extends into the retina (Figs. 7F, G) and *pax6* expression is contracted (Figs. 7H, I). These results support the hypothesis that loss of *ptc1* function is very likely to be the underlying cause of the colobomas in *blw*.

We also wanted to determine if *atp6v0b*$^{N113K}$ was causative or if it contributed to the colobomas observed in *blw*. As mentioned above, v0 subunits have been shown to be involved in mediating the release of Hedgehog-like ligands in *C. elegans* (Liegeois et al., 2006). Changes
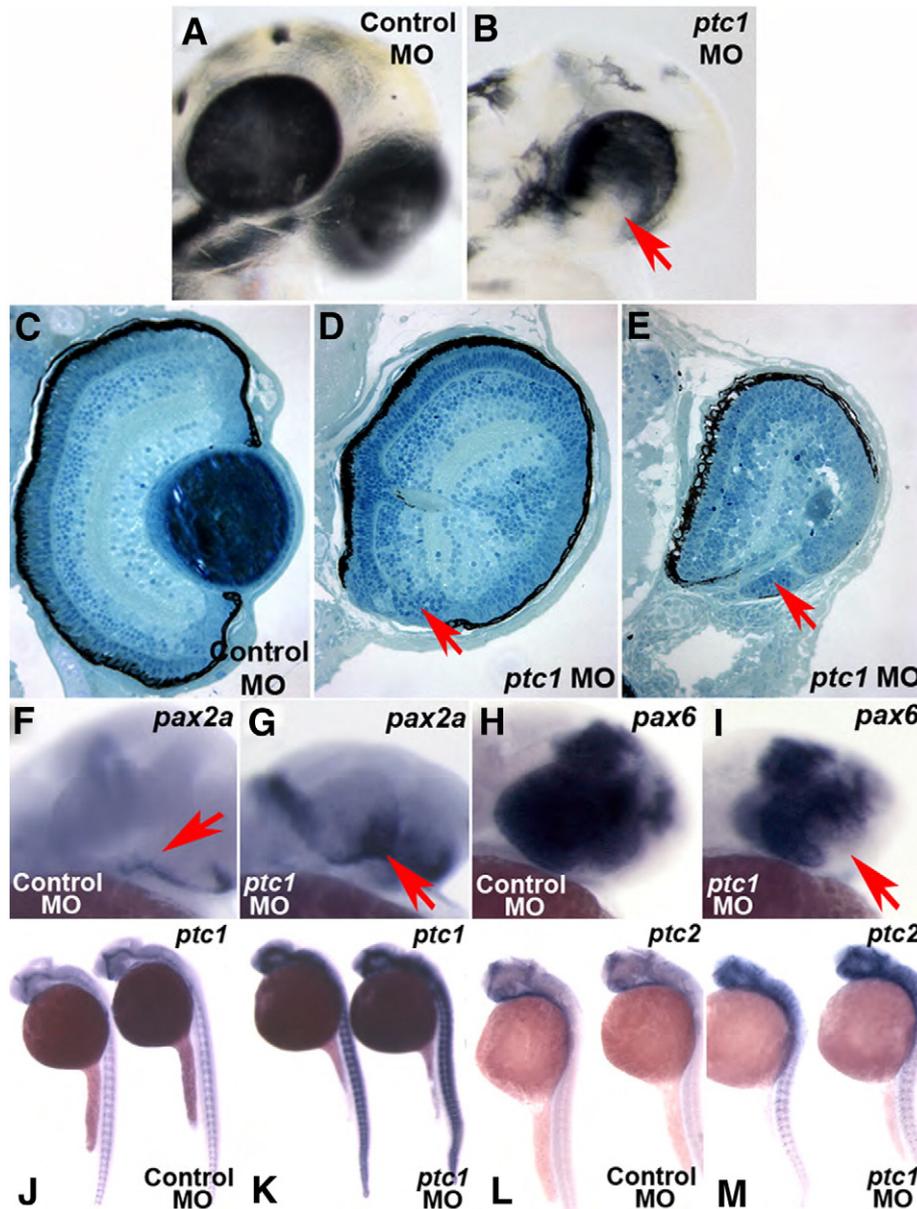


**Fig. 7.** Loss of *ptc1* leads to colobomas and ventral optic cup defects. 1.3 ng injection of a translation blocking morpholino targeting *ptc1* transcripts (*ptc1*MO) results in colobomas. Lateral views of a (A) Control morpholino (ControlMO) injected and (B) *ptc1* morphant at 2.5 dpf. Morphants possess bilateral colobomas (arrow in panel B). Morphants are more severely affected than *blw* mutants, showing medial displacement and lateral flexure of the eyes, and lens displacement. Overt brain and muscle defects are also observed. (C–E) Transverse histological sections from a 5 dpf wild-type (C) and *ptc1* morphants (D, E). Severe colobomas are obvious in the morphants (arrows in panels D, E), and in the many of them the lens is also displaced and lies out of the plane of the section. *pax2a* expression is expanded into the retina at 24 hpf (F, G) and *pax6* expression is contracted (H, I). The Hh target genes *ptc1* (J, K) and *ptc2* (L, M) also show expanded domains of expression in *ptc1* morphants.
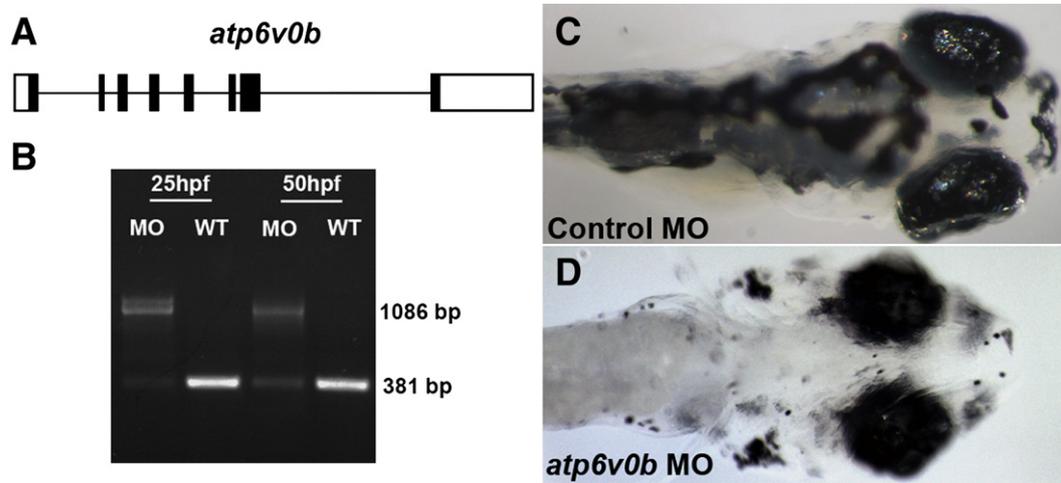
**Fig. 8.** *atp6v0b* morpholinos do not phenocopy *blowout*. (A) The *atp6v0b* predicted genomic organization. *atp6v0b* MO targets the exon1/intron1 splice junction and leads to the inclusion of a 705 bp intron1 and the introduction of a premature stop codon. (B) RT-PCR validation of splice blocking efficacy of the *atp6v0b* MO. (C) Control injected and (D) *atp6v0b* morphant (13 ng) at 5 dpf. Morphants display oculocutaneous albinism and retinal degeneration but show no signs of colobomas even at the highest doses of MO injection.

in *pax2a* and *pax6* expression are hallmark molecular readouts of Hh overexpression phenotypes in the eye and that we observe such changes in *blw* (Fig. 5) made it possible to envision a scenario whereby the $atp6v0b^{N113K}$ mutation could underlie or contribute to these ocular defects.

Five recessive mutations in different v-ATPase complex subunits have been identified in zebrafish, as well as a mutation in a v-ATPase associated protein (Amsterdam et al., 2004) and we have previously demonstrated that v-ATPase function is required for normal eye development (Gross et al., 2005). These v-ATPase roles, however, are largely in regulating RPE pigmentation, in mediating RPE/photoreceptor interactions and in regulating cell survival in the ciliary marginal zones of the retina (Nuckels, Darland and Gross, manuscript in preparation). Importantly, each of these v-ATPase mutations is a null or severe loss of function allele, and in none of these mutants are colobomas ever observed. Thus, we hypothesized that $atp6v0b^{N113K}$ was not likely to be a loss of function mutation, and we tested this hypothesis by MO interference. As expected, MO knockdown of *atp6v0b* does not lead to colobomas, and *atp6v0b* morphants do not resemble *blw* mutants (Fig. 8), rather, they resemble other v-ATPase loss of function mutants (Gross et al., 2005). Additionally, neither injection of *atp6v0b* mRNA or a BAC containing the *atp6v0b* locus into embryos derived from heterozygous *blw* incrosses was able to rescue the *blw* phenotype in these embryos (data not shown). Thus, we conclude that $atp6v0b^{N113K}$ is not a loss of function allele.

We also wanted to determine if the $atp6v0b^{N113K}$ mutation might possibly be a gain of function mutation. To test this hypothesis, we injected mRNA encoding either wild-type *atp6v0b* or $atp6v0b^{N113K}$ into wild-type 1-cell stage embryos and we assayed overall eye development and choroid fissure closure through 5 dpf. While defects in eye development were observed that included unilateral microphthalmia, mild to severe cyclopia and a small percentage of colobomas, their incidence was not significantly higher in $atp6v0b^{N113K}$ injected embryos than those injected with wild-type *atp6v0b* mRNA (data not shown). Thus, while we cannot definitively rule out the hypothesis that the $atp6v0b^{N113K}$ mutation contributes to the colobomas in *blw*, possibly acting as a modifier locus, neither the results of MO loss of function, mRNA and BAC rescue assays, nor those testing for gain of function by mRNA overexpression provide compelling support for this hypothesis.

*The expression of Hedgehog targets is expanded in blowout*

Truncation of Patched1 after the 8th transmembrane helix likely prevents it from inhibiting Smoothened, leading to an expansion of Hh
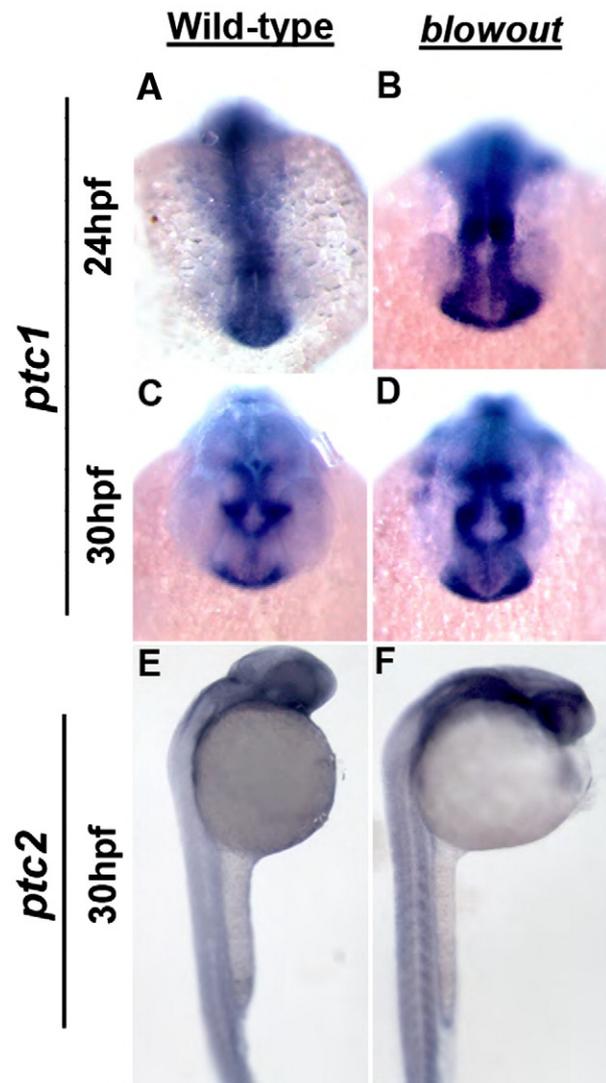


**Fig. 9.** The domains of the Hh target genes *ptc1* and *ptc2* are expanded in *blowout*. Expression of *ptc1* in the optic stalk of wild-type embryos at 24 hpf (A) and 30 hpf (C). (B, D) Expression in *blw* mutants is expanded and appears more intense at these time points both in the optic stalk, as well as in the brain and musculature (*not shown*). *ptc2* expression is also expanded in *blw* mutants (F) relative to wild-type siblings (E).

target gene expression in *blw* mutants. This model is consistent with published reports demonstrating that Hh overexpression alters gene expression in the optic stalk and optic cup in zebrafish (Ekker et al., 1995), and consistent with our observations that the expression domain of the Shh target *pax2a* is expanded in *blw* mutants and *ptc1* morphants, while the *pax6* domain is contracted (Figs. 5, 7). *ptc1* and *ptc2* are also targets of Hh pathway activation (Lewis et al., 1999; Concordet et al., 1996), likely acting in a negative feedback mechanism to limit the diffusion of the Hh morphogen and thus limit the range of Hh signaling (Chen and Struhl, 1996). To directly assess whether *ptc1* and/or *ptc2* expression is altered in *blw*, we assayed their distributions by in situ hybridization (Fig. 9). In wild-type embryos, *ptc1* is strongly expressed in the optic stalk at 24 and 30 hpf (Figs. 9A, C), as well as throughout the ventral brain and the somites (Concordet et al., 1996, and data not shown). In *blw* mutants, *ptc1* expression appears to be expanded and the message is distributed in a substantially broader domain of expression (Figs. 9B, D). Expanded domains of expression were also observed in the ventral brain and the somites (data not shown). Similarly, expansion of *ptc1* expression was also observed in *ptc1* morphants (Figs. 7J, K). Examination of *ptc2* expression in *blw* mutants yielded similar results (Figs. 9E, F), although changes in *ptc2* distribution were variable in *blw* mutants with only a subset (~40%) showing grossly obvious changes. *ptc2* expression was substantially altered in all *ptc1* morphant embryos, however (Figs. 7L, M). We highlight that while in situ hybridizations are not quantitative assays, that the *ptc1* and *ptc2* in situ signals appear to be more intense and expanded in the brain and somites in both *blw* mutant and *ptc1* morphant embryos strongly suggest that Hh pathway activity is upregulated as a result of loss of Patched1 function.

*Homozygous blowout mutants are viable and reveal post-metamorphic roles for Patched1 function in the adult zebrafish*

We were able to rear ~2–3% of homozygous *blw* mutant embryos to adulthood and the resulting fish displayed a number of obvious morphological defects (Supplemental Fig. 1). *blw* homozygotes were generally smaller in size than their heterozygous and wild-type siblings. Males and females were recovered in approximately equal numbers and fertility was normal in the homozygous mutant fish. Embryos derived from homozygous mothers continued to show variable rates of phenotypic penetrance, never reaching predicted Mendelian ratios. On average, the incidence of colobomas was approximately 35% when a homozygous female was mated with a heterozygous male, and incidences rose to over 80% when a homozygous female was mated to a homozygous male. In nearly all mutants derived from homozygous mothers that displayed colobomas, these were almost always observed bilaterally. Importantly, beyond this difference, *blw* mutants derived from homozygous mothers did not show markedly more severe or more widespread developmental defects than those derived from heterozygous mothers, indicating that there is not likely to be a significant maternal mRNA or protein rescue of the *blw* phenotype that masks defects in embryos derived from heterozygous carriers.

*Is upregulation of Hh pathway activity the mechanism that leads to colobomas in blowout?*

Given the similarities between Hh overexpression and the *blw* mutation (e.g. changes to *pax2a*, *pax6*, *ptc1* and *ptc2* expression), we next sought to directly test the hypothesis that upregulation of Hh pathway activity is the molecular mechanism underlying colobomas in *blw*. To test this hypothesis, we utilized cyclopamine, a pharmacological inhibitor of the Hh pathway that acts downstream of Patched (Cooper et al., 1998; Taipale et al., 2002), and asked whether low doses of cyclopamine were capable of suppressing colobomas in *blw* mutants. Indeed, a similar rescue paradigm has been successfully

utilized for zebrafish mutations in other negative regulators of the Hh pathway (e.g. *lep/ptc2* and *uki/Hip*; (Koudijs et al., 2005). For these assays, we took advantage of homozygous viable *blw* adults to increase the incidence of coloboma phenotypes and to abrogate the need to genotype each rescued embryo as we knew a priori that all were homozygous mutants. Low levels of cyclopamine (≤3 μM) did not lead to noticeable defects in eye development (data not shown) and thus, we assayed whether these subthreshold levels were able to suppress colobomas in *blw*. Exposure of *blw* mutants to 2 μM or 3 μM of cyclopamine between 5.5 hpf and 24 hpf was highly effective in suppressing the incidence of colobomas (Fig. 10A). In vehicle treated sibling controls, 89.8% displayed colobomas while 2 μM cyclopamine suppressed this to 26.7% and 3 μM cyclopamine to 16.7% ($p < 0.0001$; Fisher's exact test).

We next sought to determine if we could identify a window of time between 5.5 hpf and 24 hpf during which maximal rescue of colobomas in *blw* mutants could be achieved, thereby indicating the window of time when Hh signaling is likely to be required for proximal/distal patterning of the OV during normal embryogenesis. Given that 3 μM cyclopamine was able to significantly rescue colobomas in *blw* mutants (Fig. 10A), we utilized this concentration and exposed embryos over two time windows: 5.5 hpf–13 hpf and 13 hpf–24 hpf (Fig. 10B). Maximal rescue was achieved by cyclopamine exposure during the early 5.5 hpf–13 hpf window with incidences of colobomas dropping from 82% to 4% ($p < 0.0001$; Fisher's exact test). Cyclopamine exposure from 13 hpf–24 hpf resulted in 65.3% of embryos displaying colobomas ($p = 0.0278$; Fisher's exact test). While the rescue from 13 hpf to 24 hpf cyclopamine exposure is statistically significant when compared to vehicle treated controls, it is substantially lower than that achieved during the early 5.5 hpf–13 hpf window of treatment suggesting that it is during this early time window that the Hh signal is normally conveyed to the OV to segregate it into the appropriate proximal and distal territories.
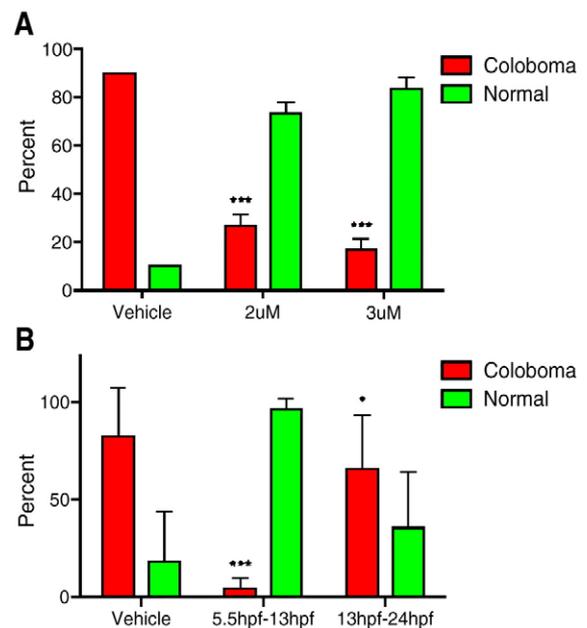


Fig. 10. Cyclopamine suppression of colobomas in *blowout*. (A) On average, 89.8% of vehicle (EtOH) treated embryos derived from homozygous incrosses displayed colobomas, while exposure of siblings to 2 μM or 3 μM cyclopamine from 5.5 hpf to 24 hpf suppressed colobomas to 26.7% and 16.7%, respectively (***$p < 0.0001$, Fisher's exact test). (B) Treatment of embryos derived from homozygous incrosses to vehicle (EtOH), or 3 μM cyclopamine from 5.5 hpf to 13 hpf, or 13 hpf to 24 hpf was also able to suppress colobomas from an average of 82% in vehicle controls to 4% in 5.5–13 hpf treated embryos (***$p < 0.0001$, Fisher's exact test), and to 65.3% in 13 hpf–24 hpf treated embryos (*$p = 0.0278$, Fisher's exact test).

## Discussion

*Blowout is a loss of function mutation in Patched1*

In this study, we have characterized zebrafish *blw*, a recessive mutation that presents with ocular coloboma and defects in retino-tectal axon pathfinding (Karlstrom et al., 1996). Positional cloning of *blw* identified two mutations; the first of these affects *ptc1*, resulting in a stop codon that truncates the Patched1 protein after the 8th transmembrane domain, and the second affects *atp6v0b*, changing a conserved asparagine residue to a lysine. MO targeting of *ptc1* transcripts results in colobomas while MO targeting of *atp6v0b* transcripts did not lead to colobomas; rather, loss of *atp6v0b* function resulted in oculocutaneous albinism and retinal degeneration. These phenotypes were identical to those observed in six other loss of function mutations in v-ATPase components or v-ATPase associated proteins, suggesting that the *atp6v0b*$^{N113K}$ mutation was not a loss of function allele (Gross et al., 2005; Nuckels et al., in preparation). Indeed, neither *atp6v0b* mRNA nor BAC injections were able to rescue or alter the ocular defects in *blw* mutants. Additionally, overexpression of *atp6v0b*$^{N113K}$ mRNA did not lead to ocular defects at a higher level than that resulting from overexpression of wild-type *atp6v0b* mRNA, also suggesting that the *atp6v0b*$^{N113K}$ mutation was not a neomorphic or gain of function allele. Thus, while we cannot exclude the possibility that *atp6v0b*$^{N113K}$ acts as a modifier of *ptc1*$^{W1040X}$, our results support a model in which the coloboma phenotypes in *blw* stem solely from a loss of Patched1 function.

Interestingly, *ptc1* morphants showed more severe ocular phenotypes than those observed in *blw* mutants. We were able to rear homozygous mutants to adulthood and embryos derived from incrosses between homozygous parents did not display more severe ocular phenotypes than those derived from heterozygous parents. This indicates that there is not a maternal supply of mRNA or protein that partially rescues the ocular phenotypes in *blw* mutants derived from heterozygous mothers. Phenotypic penetrance varies in clutches of embryos derived from heterozygous parents and while the phenotypic penetrance was higher in clutches derived from homozygous parents, they still never reached predicted ratios. These observations in conjunction with the more severe ocular phenotypes present in *ptc1* morphants suggest that the *ptc*$^{W1040X}$ mutation may be a hypomorphic partial loss of function *ptc1* allele.

While direct biochemical analysis of the truncated Ptc1$^{W1040X}$ protein will be required to test this hypothesis, should it retain some of its ability to repress Smoothened, it would be interesting with respect to other mutations that have been identified in the C-terminus of the Patched1 protein. For example, two missense mutations in the human *PATCHED1* (*PTCH*) gene have been identified that alter the C-terminal domain of PTCH (Ming et al., 2002). The first of these mutations resides in the extracellular loop between the 7th and 8th transmembrane domains of PTCH (PTCH$^{T728M}$) and the second resides in the intracellular loop between the 8th and 9th transmembrane domains of PTCH (PTCH$^{T1052M}$). Patients with these mutations display holoprosencephaly and other developmental defects, but they do not display colobomas. Interestingly, their phenotypes more closely resemble loss of function mutations in *SONIC HEDGEHOG* (*SHH*) than loss of function mutations in *PTCH*. The biochemical nature of these human mutations has not yet been characterized but given the similarity in phenotypes between them and *SHH* mutations, it may be that they disrupt the portion of the protein that is required for the inactivation of PTCH function in the presence of SHH. Thus, PTCH$^{T728M}$ and PTCH$^{T1052M}$ may act as a dominant negative such that even in the presence of SHH, these mutated proteins still represses SMOOTHENED activity and keep the Hh pathway inactive.

By comparison, truncation of the zebrafish Ptc1 protein at amino acid 1040, between the 8th and 9th intracellular loops, behaves quite differently than these point mutations. In *blw/ptc1* mutants, the Shh pathway appears to be constitutively active although with variable penetrance and relatively milder phenotypes when compared to those that arise from *Shh* overexpression (Ekker et al., 1995). It is possible that the remaining extracellular loop between the 7th and 8th transmembrane domains still retains some of its repressive ability to block Smoothened function when Hh signals are present and thus it is able to ameliorate some of the phenotypes that would be expected to arise if the Hh pathway was fully activated (i.e. to resemble *Shh* overexpression phenotypes). It is also possible that there are other redundant negative regulators of the Hh pathway that prevent full activation of the pathway in *blw/ptc1* mutants, which thereby influence the penetrance of the phenotype. Ptc2 is an ideal candidate to possess a redundant function and indeed, a recent report by Koudijs et al. (2008) demonstrates that the ocular phenotypes in *ptc1/ptc2* double mutants are much more similar to *Shh* overexpression phenotypes than those present in the single mutants.

*Ptc1-dependent regulation of Hh signaling is required for formation of the optic stalk-retina interface*

Shh signaling is a key regulator of proximal OV cell fates (Amato et al., 2004). *pax2a*, a Shh target, has been shown to directly regulate optic stalk and choroid fissure formation in the proximal OV, while *pax6* encodes a key regulatory factor involved in the specification of retina and RPE cell fates within the distal OV (Chow and Lang, 2001; Adler and Canto-Soler, 2007). In the *blw* mutant OV, the early domain of *pax2a* expression is expanded distally and *pax6* expression is contracted (Fig. 5). These results support a model in which proximal OV cell fates are expanded in *blw* mutants at the expense of distal ones, and this leads to an enlargement of the optic stalk. Indeed, these changes in gene expression in *blw* are identical to those observed from *Shh* overexpression in zebrafish, *Xenopus* and chick (Ekker et al., 1995; Macdonald et al., 1995; Perron et al., 2003; Sasagawa et al., 2002; Zhang and Yang, 2001). One problem with this model, however, is that despite the optic stalk expansion and coloboma phenotypes, later aspects of distal OV (i.e. retinal) formation are normal in *blw* mutants. One would expect that if early distal OV patterning was compromised, later retinal and RPE fates would necessarily be affected. This is not the case in *blw* mutants; retinal patterning is unaffected and overall retina size is similar to that in wild-type siblings. While we do not yet know how distal fates recover in *blw*, one possible mechanism is that the remaining *pax6* expressing distal OV is able to utilize *pax6* in a non-cell autonomous fashion (e.g. Lesaffre et al., 2007), and thereby counteract the effects of the expanded proximal *pax2a* expressing regions. In this scenario, the optic stalk would be refractory to this "rescue" and thus still expand into the choroid fissure, but the remainder of the distal OV is able to develop relatively normally. Additional analyses are required to test this hypothesis and to determine why *blw* mutants do not display distal OV defects despite the early changes in gene expression domains observed within the OV at 18 hpf.

Colobomas in *blw* were suppressed by pharmacological inhibition of Hh pathway activity indicating that it is the dysregulation of this pathway that underlies the coloboma phenotype. We suspect that colobomas result from the expansion of the optic stalk into the choroid fissure which prevents its lateral edges from meeting and fusing; however, it is also possible that overproliferation of cells within the optic stalk itself contributes to these colobomas by further expanding the optic stalk into the ventral optic cup, and thus impeding its closure. Hh signaling is known to regulate cell proliferation in a number of cellular and developmental contexts, including the eye, through the activation of key cell cycle regulators like cyclin D1, cyclin B1 and cyclin A2, as well as the phosphatase, Cdc25, that collectively function to maintain proliferative cells in the cell cycle (Adolphe et al., 2006; Agathocleous et al., 2007; Locker et al., 2006). In *blw*, an Hh-dependent dysregulation of cell proliferation may also be occurring within the

proximal OV which increases the amount of stalk tissue and thereby physically impedes closure of the choroid fissure. It will be interesting in future studies to determine if proliferation and the expression of these cell cycle components are upregulated in the optic stalk of *blw* mutants.

Hh signaling is required for later aspects of optic stalk development in mouse whereby retinal ganglion cell derived Shh is required for optic stalk neuroepithelial cells to develop into astroglia, as well as to suppress pigment cell formation around the optic nerve (Dakubo et al., 2003; Torres et al., 1996). We observed continued expression of *pax2a* mRNA in the optic stalk and ectopically in the retina of *blw* mutants when compared to that in wild-type siblings, where expression had ceased and differentiation commenced by 48 hpf. Beyond the coloboma induced morphological abnormalities in the retina of *blw* mutants, histologically and immunohistochemically their retinas appear relatively normal. That said, we do not know the effect of the mutation on later aspects of optic stalk development, as we have not yet assayed the differentiated state of the optic stalk in *blw* mutants. Based on the results in mouse, one might hypothesize that neuroepithelial cells of the *blw* optic stalk would remain undifferentiated due to the prolonged expression of these specification genes. Conversely, one might also hypothesize that the optic stalk in *blw* might differentiate but that glial cells would be overrepresented as a result of dysregulated Hh target gene expression. *blw* was originally identified based on defects in retinotectal pathfinding (Karlstrom et al., 1996), and in either of the above scenarios, retinal ganglion cell axons would likely not properly find their way to the optic nerve and/or the optic tectum. Future studies will be required to examine these possibilities and determine the molecular basis for the pathfinding defects in *blw*.

Finally, underscoring the importance of Patched-dependent regulation of Hh signaling in human disease, loss of function mutations in human *PTCH* lead to Basal Cell Naevus or Gorlin syndrome (BCNS; OMIM #109400), a developmental disorder characterized by dental, skeletal and ocular defects (Hahn et al., 1996; Johnson et al., 1996). Ocular phenotypes associated with BCNS include abnormal myelination of the optic nerve, retinal dysplasia and colobomas; however, the mechanism through which *PTCH* mutations lead to these ocular defects has not been established (Black et al., 2003; De Jong et al., 1985; Manners et al., 1996). Our results demonstrate a critical role for zebrafish Patched1 in negatively regulating Hedgehog signaling within the proximal OV and possibly in functioning to restrict Hh-dependent cell proliferation therein. BCNS-related pathologies may result from unrestricted proliferation within the retina, a model recently proposed by Black et al. (2003). That a subset of homozygous adult *blw* mutants are viable will enable us to test this hypothesis and to identify later roles for *ptc1*-dependent Hh regulation in ocular development and homeostasis, as well as to model other non-ocular BCNS associated pathologies in zebrafish.

## Acknowledgments

## Appendix A. Supplementary data

Supplementary data associated with this article can be found, in the online version, at doi:10.1016/j.ydbio.2008.03.035.

## References

Adler, R., Canto-Soler, M.V., 2007. Molecular mechanisms of optic vesicle development: complexities, ambiguities and controversies. Dev. Biol. 305, 1–13.

Adolphe, C., Hetherington, R., Ellis, T., Wainwright, B., 2006. Patched1 functions as a gatekeeper by promoting cell cycle progression. Cancer Res. 66, 2081–2088.

Agathocleous, M., Locker, M., Harris, W.A., Perron, M., 2007. A general role of hedgehog in the regulation of proliferation. Cell Cycle 6, 156–159.

Amato, M.A., Boy, S., Perron, M., 2004. Hedgehog signaling in vertebrate eye development: a growing puzzle. Cell Mol. Life Sci. 61, 899–910.

Amsterdam, A., Nissen, R.M., Sun, Z., Swindell, E.C., Farrington, S., Hopkins, N., 2004. Identification of 315 genes essential for early zebrafish development. Proc. Natl. Acad. Sci. USA 101, 12792–12797.

Barbieri, A.M., Lupo, G., Bulfone, A., Andreazzoli, M., Mariani, M., Fougerousse, F., Consalez, G.G., Borsani, G., Beckmann, J.S., Barsacchi, G., Ballabio, A., Banfi, S., 1999. A homeobox gene, vax2, controls the patterning of the eye dorsoventral axis. Proc. Natl. Acad. Sci. USA 96, 10729–10734.

Barbieri, A.M., Broccoli, V., Bovolenta, P., Alfano, G., Marchitiello, A., Mocchetti, C., Crippa, L., Bulfone, A., Marigo, V., Ballabio, A., Banfi, S., 2002. Vax2 inactivation in mouse determines alteration of the eye dorsal–ventral axis, misrouting of the optic fibres and eye coloboma. Development 129, 805–813.

Barresi, M.J., Stickney, H.L., Devoto, S.H., 2000. The zebrafish slow-muscle-omitted gene product is required for Hedgehog signal transduction and the development of slow muscle identity. Development 127, 2189–2199.

Barth, K.A., Wilson, S.W., 1995. Expression of zebrafish nk2.2 is influenced by sonic hedgehog/vertebrate hedgehog-1 and demarcates a zone of neuronal differentiation in the embryonic forebrain. Development 121, 1755–1768.

Beales, P.L., Bland, E., Tobin, J.L., Bacchelli, C., Tuysuz, B., Hill, J., Rix, S., Pearson, C.G., Kai, M., Hartley, J., Johnson, C., Irving, M., Elcioglu, N., Winey, M., Tada, M., Scambler, P.J., 2007. IFT80, which encodes a conserved intraflagellar transport protein, is mutated in Jeune asphyxiating thoracic dystrophy. Nat. Genet. 39, 727–729.

Bertuzzi, S., Hindges, R., Mui, S.H., O'Leary, D.D., Lemke, G., 1999. The homeodomain protein vax1 is required for axon guidance and major tract formation in the developing forebrain. Genes Dev. 13, 3092–3105.

Black, G.C., Mazerolle, C.J., Wang, Y., Campsall, K.D., Petrin, D., Leonard, B.C., Damji, K.F., Evans, D.G., McLeod, D., Wallace, V.A., 2003. Abnormalities of the vitreoretinal interface caused by dysregulated Hedgehog signaling during retinal development. Hum. Mol. Genet. 12, 3269–3276.

Chang, L., Blain, D., Bertuzzi, S., Brooks, B.P., 2006. Uveal coloboma: clinical and basic science update. Curr. Opin. Ophthalmol. 17, 447–470.

Chen, Y., Struhl, G., 1996. Dual roles for patched in sequestering and transducing Hedgehog. Cell 87, 553–563.

Chiang, C., Litingtung, Y., Lee, E., Young, K.E., Corden, J.L., Westphal, H., Beachy, P.A., 1996. Cyclopia and defective axial patterning in mice lacking Sonic hedgehog gene function. Nature 383, 407–413.

Chow, R.L., Lang, R.A., 2001. Early eye development in vertebrates. Annu. Rev. Cell Dev. Biol. 17, 255–296.

Concordet, J.P., Lewis, K.E., Moore, J.W., Goodrich, L.V., Johnson, R.L., Scott, M.P., Ingham, P.W., 1996. Spatial regulation of a zebrafish patched homologue reflects the roles of sonic hedgehog and protein kinase A in neural tube and somite patterning. Development 122, 2835–2846.

Cooper, M.K., Porter, J.A., Young, K.E., Beachy, P.A., 1998. Teratogen-mediated inhibition of target tissue response to Shh signaling. Science 280, 1603–1607.

Dakubo, G.D., Wang, Y.P., Mazerolle, C., Campsall, K., McMahon, A.P., Wallace, V.A., 2003. Retinal ganglion cell-derived sonic hedgehog signaling is required for optic disc and stalk neuroepithelial cell development. Development 130, 2967–2980.

De Jong, P.T., Bistervels, B., Cosgrove, J., de Grip, G., Leys, A., Goffin, M., 1985. Medullated nerve fibers. A sign of multiple basal cell nevi (Gorlin's) syndrome. Arch. Ophthalmol. 103, 1833–1836.

Dutta, S., Dietrich, J.E., Aspock, G., Burdine, R.D., Schier, A., Westerfield, M., Varga, Z.M., 2005. pitx3 defines an equivalence domain for lens and anterior pituitary placode. Development 132, 1579–1590.

Ekker, S.C., Ungar, A.R., Greenstein, P., von Kessler, D.P., Porter, J.A., Moon, R.T., Beachy, P.A., 1995. Patterning activities of vertebrate hedgehog proteins in the developing eye and brain. Curr. Biol. 5, 944–955.

Esteve, P., Bovolenta, P., 2006. Secreted inducers in vertebrate eye development: more functions for old morphogens. Curr. Opin. Neurobiol. 16, 13–19.

Fitzpatrick, D.R., van Heyningen, V., 2005. Developmental eye disorders. Curr. Opin. Genet. Dev. 15, 348–353.

Goldsmith, P., Harris, W.A., 2003. The zebrafish as a tool for understanding the biology of visual systems. Semin. Cell Dev. Biol. 14, 11–18.

Gregory-Evans, C.Y., Williams, M.J., Halford, S., Gregory-Evans, K., 2004. Ocular coloboma: a reassessment in the age of molecular neuroscience. J. Med. Genet. 41, 881–891.

Gross, J.M., Dowling, J.E., 2005. Tbx2b is essential for neuronal differentiation along the dorsal/ventral axis of the zebrafish retina. Proc. Natl Acad. Sci. USA 102, 4371–4376.

Gross, J.M., Perkins, B.D., 2008. Zebrafish mutants as models for congenital ocular disorders in humans. Mol. Reprod. Dev. 75, 547–555.

Gross, J.M., Perkins, B.D., Amsterdam, A., Egana, A., Darland, T., Matsui, J.I., Sciascia, S., Hopkins, N., Dowling, J.E., 2005. Identification of zebrafish insertional mutants with defects in visual system development and function. Genetics 170, 245–261.

Hahn, H., Wicking, C., Zaphiropoulous, P.G., Gailani, M.R., Shanley, S., Chidambaram, A., Vorechovsky, I., Holmberg, E., Unden, A.B., Gillies, S., Negus, K., Smyth, I., Pressman, C., Leffell, D.J., Gerrard, B., Goldstein, A.M., Dean, M., Toftgard, R., Chenevix-Trench, G., Wainwright, B., Bale, A.E., 1996. Mutations of the human homolog of *Drosophila* patched in the nevoid basal cell carcinoma syndrome. Cell 85, 841–851.

Hallonet, M., Hollemann, T., Wehr, R., Jenkins, N.A., Copeland, N.G., Pieler, T., Gruss, P., 1998. Vax1 is a novel homeobox-containing gene expressed in the developing anterior ventral forebrain. Development 125, 2599–2610.

Hallonet, M., Hollemann, T., Pieler, T., Gruss, P., 1999. Vax1, a novel homeobox-containing gene, directs development of the basal forebrain and visual system. Genes Dev. 13, 3106–3114.

Heisenberg, C.P., Brennan, C., Wilson, S.W., 1999. Zebrafish aussicht mutant embryos exhibit widespread overexpression of ace (fgf8) and coincident defects in CNS development. Development 126, 2129–2140.

Hiesinger, P.R., Fayyazuddin, A., Mehta, S.Q., Rosenmund, T., Schulze, K.L., Zhai, R.G., Verstreken, P., Cao, Y., Zhou, Y., Kunz, J., Bellen, H.J., 2005. The v-ATPase V0 subunit a1 is required for a late step in synaptic vesicle exocytosis in Drosophila. Cell 121, 607–620.

Hero, I., Farjah, M., Scholtz, C.L., 1991. The prenatal development of the optic fissure in colobomatous microphthalmia. Invest. Ophthalmol. Vis. Sci. 32, 2622–2635.

Johnson, R.L., Rothman, A.L., Xie, J., Goodrich, L.V., Bare, J.W., Bonifas, J.M., Quinn, A.G., Myers, R.M., Cox, D.R., Epstein Jr., E.H., Scott, M.P., 1996. Human homolog of patched, a candidate gene for the basal cell nevus syndrome. Science 272, 1668–1671.

Jowett, T., Lettice, L., 1994. Whole-mount in situ hybridizations on zebrafish embryos using a mixture of digoxigenin- and fluorescein-labelled probes. Trends Genet. 10, 73–74.

Karlstrom, R.O., Trowe, T., Klostermann, S., Baier, H., Brand, M., Crawford, A.D., Grunewald, B., Haffter, P., Hoffmann, H., Meyer, S.U., Muller, B.K., Richter, S., van Eeden, F.J., Nusslein-Volhard, C., Bonhoeffer, F., 1996. Zebrafish mutations affecting retinotectal axon pathfinding. Development 123, 427–438.

Karlstrom, R.O., Talbot, W.S., Schier, A.F., 1999. Comparative synteny cloning of zebrafish you-too: mutations in the Hedgehog target gli2 affect ventral forebrain patterning. Genes Dev. 13, 388–393.

Kim, T.H., Goodman, J., Anderson, K.V., Niswander, L., 2007. Phactr4 regulates neural tube and optic fissure closure by controlling PP1-, Rb-, and E2F1-regulated cell-cycle progression. Dev. Cell 13, 87–102.

Kontani, K., Moskowitz, I.P., Rothman, J.H., 2005. Repression of cell–cell fusion by components of the C. elegans vacuolar ATPase complex. Dev. Cell 8, 787–794.

Koudijs, M.J., den Broeder, M.J., Keijser, A., Wienholds, E., Houwing, S., van Rooijen, E.M., Geisler, R., van Eeden, F.J., 2005. The zebrafish mutants dre, uki, and lep encode negative regulators of the hedgehog signaling pathway. PLoS Genet. 1, e19.

Koudijs, M.J., den Broeder, M.J., Groot, E., van Eeden, F.J., 2008. Genetic analysis of two zebrafish patched homologues identifies novel roles for the hedgehog signaling pathway. BMC Dev. Biol. 8, 15.

Lee, J., Gross, J.M., 2007. Laminin {beta}1 and {gamma}1 containing laminins are essential for basement membrane integrity in the zebrafish eye. Invest. Ophthalmol. Vis. Sci. 48, 2483–2490.

Lesaffre, B., Joliot, A., Prochiantz, A., Volovitch, M., 2007. Direct non-cell autonomous Pax6 activity regulates eye development in the zebrafish. Neural. Develop. 2, 2.

Lewis, K.E., Concordet, J.P., Ingham, P.W., 1999. Characterisation of a second patched gene in the zebrafish Danio rerio and the differential response of patched genes to Hedgehog signalling. Dev. Biol. 208, 14–29.

Liegeois, S., Benedetto, A., Garnier, J.M., Schwab, Y., Labouesse, M., 2006. The V0-ATPase mediates apical secretion of exosomes containing Hedgehog-related proteins in Caenorhabditis elegans. J. Cell Biol. 173, 949–961.

Locker, M., Agathocleous, M., Amato, M.A., Parain, K., Harris, W.A., Perron, M., 2006. Hedgehog signaling and the retina: insights into the mechanisms controlling the proliferative properties of neural precursors. Genes Dev. 20, 3036–3048.

Macdonald, R., Barth, K.A., Xu, Q., Holder, N., Mikkola, I., Wilson, S.W., 1995. Midline signalling is required for Pax gene regulation and patterning of the eyes. Development 121, 3267–3278.

Macdonald, R., Scholes, J., Strahle, U., Brennan, C., Holder, N., Brand, M., Wilson, S.W., 1997. The Pax protein Noi is required for commissural axon pathway formation in the rostral forebrain. Development 124, 2397–2408.

Manners, R.M., Morris, R.J., Francis, P.J., Hatchwell, E., 1996. Microphthalmos in association with Gorlin's syndrome. Br. J. Ophthalmol. 80, 378.

Ming, J.E., Kaupas, M.E., Roessler, E., Brunner, H.G., Golabi, M., Tekin, M., Stratton, R.F., Sujansky, E., Bale, S.J., Muenke, M., 2002. Mutations in PATCHED-1, the receptor for SONIC HEDGEHOG, are associated with holoprosencephaly. Hum. Genet. 110, 297–301.

Mui, S.H., Hindges, R., O'Leary, D.D., Lemke, G., Bertuzzi, S., 2002. The homeodomain protein Vax2 patterns the dorsoventral and nasotemporal axes of the eye. Development 129, 797–804.

Mui, S.H., Kim, J.W., Lemke, G., Bertuzzi, S., 2005. Vax genes ventralize the embryonic eye. Genes Dev. 19, 1249–1259.

Nakayama, Y., Miyake, A., Nakagawa, Y., Mido, T., Yoshikawa, M., Konishi, M., Itoh, N., 2008. Fgf19 is required for zebrafish lens and retina development. Dev. Biol. 313, 752–766.

Nelson, N., Harvey, W.R., 1999. Vacuolar and plasma membrane proton-adenosine-triphosphatases. Physiol. Rev. 79, 361–385.

Neuhauss, S.C., Biehlmaier, O., Seeliger, M.W., Das, T., Kohler, K., Harris, W.A., Baier, H., 1999. Genetic disorders of vision revealed by a behavioral screen of 400 essential loci in zebrafish. J. Neurosci. 19, 8603–8615.

Nishi, T., Forgac, M., 2002. The vacuolar (H+)-ATPases—nature's most versatile proton pumps. Nat. Rev. Mol. Cell Biol. 3, 94–103.

Ohsaki, K., Morimitsu, T., Ishida, Y., Kominami, R., Takahashi, N., 1999. Expression of the Vax family homeobox genes suggests multiple roles in eye development. Genes Cells 4, 267–276.

Otteson, D.C., Shelden, E., Jones, J.M., Kameoka, J., Hitchcock, P.F., 1998. Pax2 expression and retinal morphogenesis in the normal and Krd mouse. Dev. Biol. 193, 209–224.

Perron, M., Boy, S., Amato, M.A., Viczian, A., Koebernick, K., Pieler, T., Harris, W.A., 2003. A novel function for Hedgehog signalling in retinal pigment epithelium differentiation. Development 130, 1565–1577.

Roessler, E., Belloni, E., Gaudenz, K., Jay, P., Berta, P., Scherer, S.W., Tsui, L.C., Muenke, M., 1996. Mutations in the human Sonic Hedgehog gene cause holoprosencephaly. Nat. Genet. 14, 357–360.

Sanyanusin, P., Schimmenti, L.A., McNoe, L.A., Ward, T.A., Pierpont, M.E., Sullivan, M.J., Dobyns, W.B., Eccles, M.R., 1995. Mutation of the PAX2 gene in a family with optic nerve colobomas, renal anomalies and vesicoureteral reflux. Nat. Genet. 9, 358–364.

Sasagawa, S., Takabatake, T., Takabatake, Y., Muramatsu, T., Takeshima, K., 2002. Axes establishment during eye morphogenesis in Xenopus by coordinate and antagonistic actions of BMP4, Shh, and RA. Genesis 33, 86–96.

Schauerte, H.E., van Eeden, F.J., Fricke, C., Odenthal, J., Strahle, U., Haffter, P., 1998. Sonic hedgehog is not required for the induction of medial floor plate cells in the zebrafish. Development 125, 2983–2993.

Schwarz, M., Cecconi, F., Bernier, G., Andrejewski, N., Kammandel, B., Wagner, M., Gruss, P., 2000. Spatial specification of mammalian eye territories by reciprocal transcriptional repression of Pax2 and Pax6. Development 127, 4325–4334.

Taipale, J., Cooper, M.K., Maiti, T., Beachy, P.A., 2002. Patched acts catalytically to suppress the activity of Smoothened. Nature 418, 892–897.

Take-uchi, M., Clarke, J.D., Wilson, S.W., 2003. Hedgehog signalling maintains the optic stalk-retinal interface through the regulation of Vax gene activity. Development 130, 955–968.

Torres, M., Gomez-Pardo, E., Gruss, P., 1996. Pax2 contributes to inner ear patterning and optic nerve trajectory. Development 122, 3381–3391.

Varga, Z.M., Amores, A., Lewis, K.E., Yan, Y.L., Postlethwait, J.H., Eisen, J.S., Westerfield, M., 2001. Zebrafish smoothened functions in ventral neural tube specification and axon tract formation. Development 128, 3497–3509.

Willer, G.B., Lee, V.M., Gregg, R.G., Link, B.A., 2005. Analysis of the Zebrafish perplexed mutation reveals tissue-specific roles for de novo pyrimidine synthesis during development. Genetics 170, 1827–1837.

Wolff, C., Roy, S., Ingham, P.W., 2003. Multiple muscle cell identities induced by distinct levels and timing of hedgehog activity in the zebrafish embryo. Curr. Biol. 13, 1169–1181.

Yamamoto, Y., Stock, D.W., Jeffery, W.R., 2004. Hedgehog signalling controls eye degeneration in blind cavefish. Nature 431, 844–847.

Zhang, X.M., Yang, X.J., 2001. Temporal and spatial effects of Sonic hedgehog signaling in chick eye morphogenesis. Dev. Biol. 233, 271–290.